Development 134, 4167-4176 (2007) doi:10.1242/dev.010702

Synaptic differentiation is defective in mice lacking acetylcholine receptor β-subunit tyrosine phosphorylation

Matthew B. Friese, Chris S. Blagden and Steven J. Burden*

Agrin activates MuSK, a receptor tyrosine kinase expressed in skeletal muscle, leading to tyrosine phosphorylation of the acetylcholine receptor (AChR) β-subunit and clustering of AChRs. The importance of AChR β-subunit tyrosine phosphorylation in clustering AChRs and regulating synaptic differentiation is poorly understood. We generated mice with targeted mutations in the three intracellular tyrosines of the AChR β-subunit (*AChR-β$^{3F/3F}$*). Mice lacking AChR β-subunit tyrosine phosphorylation thrive postnatally and have no overt behavioral defects, indicating that AChR β-subunit tyrosine phosphorylation is not essential for the formation of neuromuscular synapses. Nonetheless, the size of synapses and the density of synaptic AChRs are reduced in *AChR-β$^{3F/3F}$* mutant mice. Moreover, synapses are structurally simplified and the organization of postjunctional folds is aberrant in mice lacking tyrosine phosphorylation of the AChR β-subunit. Furthermore, mutant AChRs cluster poorly in response to agrin and are readily extracted from the cell surface of cultured myotubes by non-ionic detergent. These data indicate that tyrosine phosphorylation of the AChR β-subunit has an important role in organizing AChRs and regulating synaptic differentiation.

KEY WORDS: AChR clustering, Junctional folds, Neuromuscular junction, Synaptogenesis, *Chrnb1*

INTRODUCTION

Numerous ligand-gated channels, including receptors for glutamate, γ-amino butyric acid and acetylcholine, are tyrosine phosphorylated in vivo, but the role of this post-translational modification in neurotransmitter receptor function is poorly understood (Huganir et al., 1984; Qu et al., 1990; Moon et al., 1994; Wan et al., 1997; Swope et al., 1999). The nicotinic acetylcholine receptor (AChR) is a pentamer composed of four different subunits, and two of these subunits, β and δ, are tyrosine phosphorylated in vivo (Qu et al., 1990; Mittaud et al., 2001). Tyrosine phosphorylation of the AChR is stimulated by agrin, a ~200 kDa protein that is synthesized by motor neurons and released from nerve terminals (Wallace et al., 1991). Agrin stimulates MuSK, a muscle-specific receptor tyrosine kinase that is concentrated in the postsynaptic membrane and critical for synapse formation (DeChiara et al., 1996; Glass et al., 1996). Activation of MuSK leads to the rapid tyrosine phosphorylation and subsequently to the clustering of AChRs. In mice lacking MuSK, AChRs are expressed, but they are neither tyrosine phosphorylated nor clustered (DeChiara et al., 1996; Glass et al., 1996; Smith et al., 2001). Taken together, these findings suggest that AChR tyrosine phosphorylation may have an important and possibly requisite role in clustering AChRs at synapses.

Consistent with this notion, prior studies, which analyzed transfected wild-type cultured myotubes reported that mutant AChR pentamers, which contain a β-subunit that cannot be tyrosine phosphorylated, cluster two-fold less efficiently than wild-type AChRs (Meyer and Wallace, 1998; Borges and Ferns, 2001). In addition, these mutant AChRs are extracted more readily than wild-type AChRs with a non-ionic detergent (Borges and Ferns, 2001). These data indicate that tyrosine phosphorylation of the AChR β-subunit has a role in clustering and stabilizing AChRs in cultured myotubes, but the role of AChR tyrosine phosphorylation in synaptic differentiation has not been studied.

To determine the role of AChR β tyrosine phosphorylation in clustering and anchoring AChRs at synapses, we generated mice with targeted mutations in the three tyrosines in the large intracellular loop of the AChR β-subunit. Mice lacking AChR β-subunit tyrosine phosphorylation survive postnatally, but their neuromuscular synapses are simplified and contain a reduced number of AChRs, indicating that tyrosine phosphorylation of the AChR β-subunit has an important role in organizing and stabilizing AChRs at synapses.

MATERIALS AND METHODS

Gene targeting construct and generation of *AChR-β$^{3F/3F}$* mice

The *Chrnb1* gene was isolated from a mouse genomic BAC library (Research Genetics, Huntsville, AL) by screening for exon 10 using a PCR assay. A 8.5 kb *Hin*dIII fragment, extending from intron 7 to intron 11 of the *Chrnb1* locus was subcloned, and a 7.8 kb *Xba*I-*Xho*I fragment was used to construct a targeting vector (Fig. 1A). PCR mutagenesis was used to convert codon 357 from TAC to TTC, codon 390 from TAT to TTT, and codon 442 from TAC to TTC (accession number M14537). Although substitution of these tyrosine residues with phenylalanine prevents phosphorylation, we cannot exclude the possibility that the tyrosine hydroxyl groups serve a different function and that removal of these hydroxyl groups leads to defects unrelated to phosphorylation. An *frt*-flanked PGK-neomycin resistance cassette was cloned into an *Eco*RV site, which we introduced in intron 10, and a β-actin-diphtheria toxin A cassette was introduced at the 3′-end of the genomic fragment to create the targeting construct (Fig. 1A). Nucleis (Lyon, France) performed the ES cell electroporation, ES cell screening and blastocyst injections. 384 G418-resistant clones were isolated; a PCR assay (one primer in neo, CCGGCAAGTTCCTATTCTC, and one primer 3′ to the targeting construct, TACACAACAAGCTCCAGG) identified 16 clones in which the targeting construct recombined into the AChR β locus. Gene targeting in 10 clones was verified by probing Southern blots of *Hin*dIII-digested genomic DNA with a *Hin*dIII-*Xho*I fragment (Fig. 1B). In addition, exons 10 and 11 were sequenced to ensure that recombination did not occur between the neo cassette and Y357; this analysis demonstrated that four clones contained the three desired tyrosine to phenylalanine mutations. Three targeted ES cell lines were injected into blastocysts. One of the lines

Molecular Neurobiology Program, The Helen L. and Martin S. Kimmel Center for Biology and Medicine at the Skirball Institute of Biomolecular Medicine, NYU Medical School, 540 First Avenue, New York, NY 10016, USA.

*Author for correspondence (e-mail: burden@saturn.med.nyu.edu)

Accepted 11 September 2007

(3B4) produced chimeric offspring and was subsequently outcrossed to C57BL6 mice. The *frt*-flanked neo cassette was excised by further mating to FLPE mice (Jackson Laboratory, Bar Harbor, ME, USA), and the mice were genotyped by PCR (CCCGGACCTGCGACGATTTA; ACTAGGGTCCCGACGCTTGT).

Isolation of AChR complexes

Whole leg muscles from P0 mice were homogenized in lysis buffer [50 mM sodium chloride, 30 mM triethanolamine pH 7.5, 50 mM sodium flouride, 5 mM EDTA, 5 mM EGTA, 2 mM sodium orthovanadate, 1 mM *N*-ethylmaleimide, 1 mM sodium tetrathionate, 1 μg/ml pepstatin plus Complete protease inhibitors (Roche, Basel, Switzerland)] with a PT 10/35 Polytron (Kinematica AG, Littau-Lucerne, Switzerland) at 4°C. NP-40 was added to a final concentration of 1%, and the extract was incubated with rocking for 30 minutes at 4°C. Insoluble proteins were removed by centrifugation, and the supernatant was pre-cleared for 1 hour at 4°C against streptavidin-agarose (Sigma, St Louis, MO). The supernatant was collected and incubated for 1 hour at 4°C with biotinylated-α-bungarotoxin (α-BGT; Invitrogen, Carlsbad, CA, USA). AChR complexes were precipitated overnight with streptavidin-agarose, followed by washing (three washes for 3 minutes each) in lysis buffer containing 1% NP-40. Western blots were probed with antibodies to phosphotyrosine (4G10, 1:1000; Upstate USA, Charlottesville, VA). The blots were subsequently stripped and reprobed with antibodies to the AChR β-subunit (mAb124, 1:5000; a gift from J. Lindstrom, University of Pennsylvania, Philadelphia, PA).

AChR surface expression

P0 mouse diaphragms were dissected, and AChRs were labeled with 20 nM ^{125}I-α-BGT (Perkin Elmer, Waltham, MA) for 1 hour at 37°C in oxygenated L15 medium. Background binding, in the presence of 10 μM non-radioactive α-BGT, was ~10% of the binding without competitor. Muscles were washed (five washes for 50 minutes) in oxygenated L15 medium. Bound ^{125}I-α-BGT was measured in a Wallac 1470 gamma counter (Perkin Elmer), and the muscle was weighed.

Immunostaining sections and whole mounts of muscle

Tibialis anterior muscles from P30 mice were mildly fixed (in 0.1% paraformaldehyde in PBS) for 1 hour at 4°C, rinsed twice at 4°C in PBS, cryoprotected (in 30% sucrose-PBS) overnight at 4°C, and embedded in TissueTek (Sakura, Tokyo, Japan). Frozen sections (10 μm) were stained with the following antibodies: p-AchRβ1-Tyr 390 (1:200; sc-17087; Santa Cruz Biotechnology, Santa Cruz, CA), MuSK (1:1000; #83033), rapsyn (1:500; #232), APC (1:200; sc-895 Santa Cruz Biotechnology), Abl (1:200; sc-131 Santa Cruz Biotechnology), utrophin (1:10; Vector Labs, Burlingame, CA) and dystroglycan (1:100; gift from Kevin Campbell, University of Iowa, Iowa City, IA), and AChRs were labeled with Alexa Fluor 594-α-BGT (Invitrogen). The images were acquired with a 63× (1.4 NA) objective. AChRs, axons and nerve terminals from P0 and P30 diaphragms were stained, and synaptic AChR levels and size were measured as described previously (Jaworski and Burden, 2006). Briefly, we stained diaphragm muscle with Alexa Fluor 594-α-BGT, collected confocal image stacks at the same sub-saturating amplifier gain for both genotypes using a 40× (1.3 NA) objective, and measured the Alexa Fluor 594-α-BGT-stained area. We quantified actual levels from unprocessed images but adjusted image levels for display purposes. Quantification of the pattern (stripes and gaps) of AChR staining at individual synapses and assignment to one of three categories was done initially without knowledge of the genotype; after the data were acquired, using a 63× (1.4 NA) objective, the genotype was identified.

Electron microscopy

Levator auris muscles in terminally anesthetized mice were exposed and injected with 10 μg/ml tetrodotoxin in PBS to prevent muscle contraction, and subsequently fixed in vivo with 4% paraformaldehyde/1% glutaraldehyde in 110 mM sodium phosphate buffer, pH 7.3. After dissection, fixation was allowed to continue at room temperature for 90 minutes. The muscle was washed (five times for 25 minutes) in iso-osmotic phosphate buffer (150 mM sodium chloride, 5 mM potassium chloride, 10 mM sodium phosphate, pH 7.3), and subsequently stained for acetylcholinesterase activity to locate the muscle area containing synapses (Karnovsky and Roots, 1964). Following three washes (for 15 minutes) with 100 mM Tris, pH 7.2, 160 mM sucrose, the muscle was washed again (five washes for 25 minutes) in isosmotic phosphate buffer. Following treatment with osmium (4% osmium tetroxide in 140 mM sodium phosphate, pH 7.3) for 1 hour, the muscle was washed (twice for 1 hour) in water. The muscle was stained en bloc with saturated uranyl acetate for 1 hour, dehydrated in ethanol and embedded in Epon.

Electrophysiology

Diaphragm muscles from P30 mice were dissected in oxygenated high Mg^{2+}-low Ca^{2+} Tyrode's solution (125 mM sodium chloride, 5.37 mM potassium chloride, 24 mM sodium bicarbonate, 12 mM magnesium chloride, 0.5 mM calcium chloride and 5% dextrose). Glass microelectrodes were pulled with a Sutter P-2000 micropipette puller (Novato, CA) and filled with 3 M potassium chloride to give a resistance of between 40-60 MV. Recordings of miniature end-plate potential (mepp) amplitude were made with a Dagan IX-1 (Minneapolis, MN) intracellular preamplifier connected to an ADInstruments Powerlab 8/30 data acquisition system (Colorado Springs, CO). Muscle fibers were impaled near the endplate, and the average rise-time (baseline to peak) was statistically similar and less than 3 mseconds for both genotypes. Mepp recordings were only made from fibers with resting membrane potentials between –70 and –85 mV and deviated no more than 15% during the duration of the recording. The data represent at least 30 mepps per muscle fiber.

Isolation of immortalized muscle cells

We isolated two immortalized muscle cell lines from wild-type mice that carried the H-2Kb-tsA58 transgene and two muscle lines from the *Chrnb1* mutant (hereafter referred to as *AChR-β$^{3F/3F}$*) mice that carried the H-2Kb-tsA58 transgene (Jat et al., 1991). Muscle cells were grown as described previously (Smith et al., 2001).

AChR clustering assay

Myotubes were treated for 16 hours with 500 pM agrin (R&D, Minneapolis, MN), rinsed three times (in PBS) and fixed for 10 minutes (1% paraformaldehyde in PBS). After washing (twice for 10 minutes in PBS), the muscle was incubated in 0.1 M glycine (in PBS) for 10 minutes rinsed twice in PBS and incubated for 30 minutes in 1% BSA in PBS. AChRs were labeled with Alexa Fluor 594-α-BGT (Invitrogen; 1:1000, in 1% BSA-PBS) for 1 hour and washed (three washes for 30 minutes in PBS). Myotubes were permeabilized (in PBS containing 0.1% Triton X-100) for 5 minutes and stained with Alexa Fluor 488-phalloidin (1:250; Invitrogen) (in 1% BSA-PBS) for 20 minutes to label actin. Myotubes were washed (three washes for 15 minutes in PBS) and mounted in VectaShield (Vector Labs). Images of phalloidin-stained myofibers were collected using a Zeiss LSM 510 microscope (Oberkochen, Germany), with a 20× (0.7 NA) objective, and the number and size of AChR clusters in these myotubes was determined using the Volocity (Improvision, Lexington, MA) software package. The data represent the average from two cell lines for each genotype.

AChR extraction

Differentiated myotubes were treated with 500 pM agrin in culture medium for 3 hours at 37°C. ^{125}I-α-BGT was added to fresh medium containing 500 pM agrin. Myotubes were incubated for a further 1 hour at 37°C and washed (three washes for 15 minutes in oxygenated L15 medium). AChRs were extracted by incubating myotubes in L15 medium containing 0.05% Triton X-100; the extraction solution was collected and replaced every 2 minutes for a total of 6 minutes. The remaining, unextracted AChRs were collected by incubating myotubes in L15 medium containing 1% SDS. The amount of AChR extracted with Triton X-100 and SDS was measured in a gamma counter. The data represent the average from two cell lines for each genotype. In some experiments, myotubes were pretreated with 20 nM staurosporine (Sigma) or vehicle (0.002% DMSO) for 16 hours prior to treating the myotubes with agrin.

Statistics

Statistical analyses were performed using Minitab 15 (Minitab, State College, PA). All values are given as mean±standard error. Parametric tests were used only when the data were normally distributed as

determined by the Kolmogorov-Smirnov test. Non-normal data were analyzed using the appropriate nonparametric test as indicated in the figure legend.

RESULTS

Generation of mutant mice lacking tyrosine residues in the main intracellular loop of the AChR β-subunit

Previous studies showed that agrin stimulates phosphorylation of a single tyrosine residue, Y390, in the AChR β-subunit (Borges and Ferns, 2001). Because we were concerned that the two other tyrosine residues (Y357, Y442) in the main intracellular loop of the AChR β-subunit might be phosphorylated if phosphorylation of Y390 were prevented, we used site-directed mutagenesis and homologous recombination in ES cells to replace all three tyrosine residues in the main intracellular loop with phenylalanine (Fig. 1A,B; Materials and methods). We confirmed gene targeting by PCR, Southern blotting and DNA sequencing (Fig. 1B and data not shown). Mice lacking these tyrosine phosphorylation sites (*AChR-β$^{3F/3F}$*) are born alive, nurse normally, and are otherwise indistinguishable from wild-type littermates (see Fig. S1 in the supplementary material).

To determine whether mutation of these three tyrosine residues prevents AChR β-subunit tyrosine phosphorylation, we labeled AChRs in detergent lysates from P0 limb muscles with biotinylated-α-bungarotoxin (α-BGT), isolated AChR complexes with streptavidin-agarose and probed western blots with antibodies to phosphotyrosine. Fig. 1C shows that AChRs in *AChR-β$^{3F/3F}$* mutant mice, unlike AChRs in control mice, are not tyrosine phosphorylated. In addition, we stained frozen sections of muscle from wild-type and *AChR-β$^{3F/3F}$* mutant mice with antibodies against a phosphopeptide specific to AChR-β$^{Y390\text{-}P}$ and found that these antibodies label synaptic sites in wild-type but not *AChR-β$^{3F/3F}$* mutant mice (Fig. 1D). Taken together, these data indicate that tyrosine phosphorylation of the AChR β-subunit is eliminated in *AChR-β$^{3F/3F}$* mice.

Synapses are smaller and contain fewer AChRs in *AChR-β$^{3F/3F}$* mice

AChRs at embryonic synapses are arranged in small ovoid plaques of uniform AChR density (Sanes and Lichtman, 2001). To determine whether synapse formation is impaired in *AChR-β$^{3F/3F}$* mice, we stained whole mounts of diaphragm muscle from P0 mice with

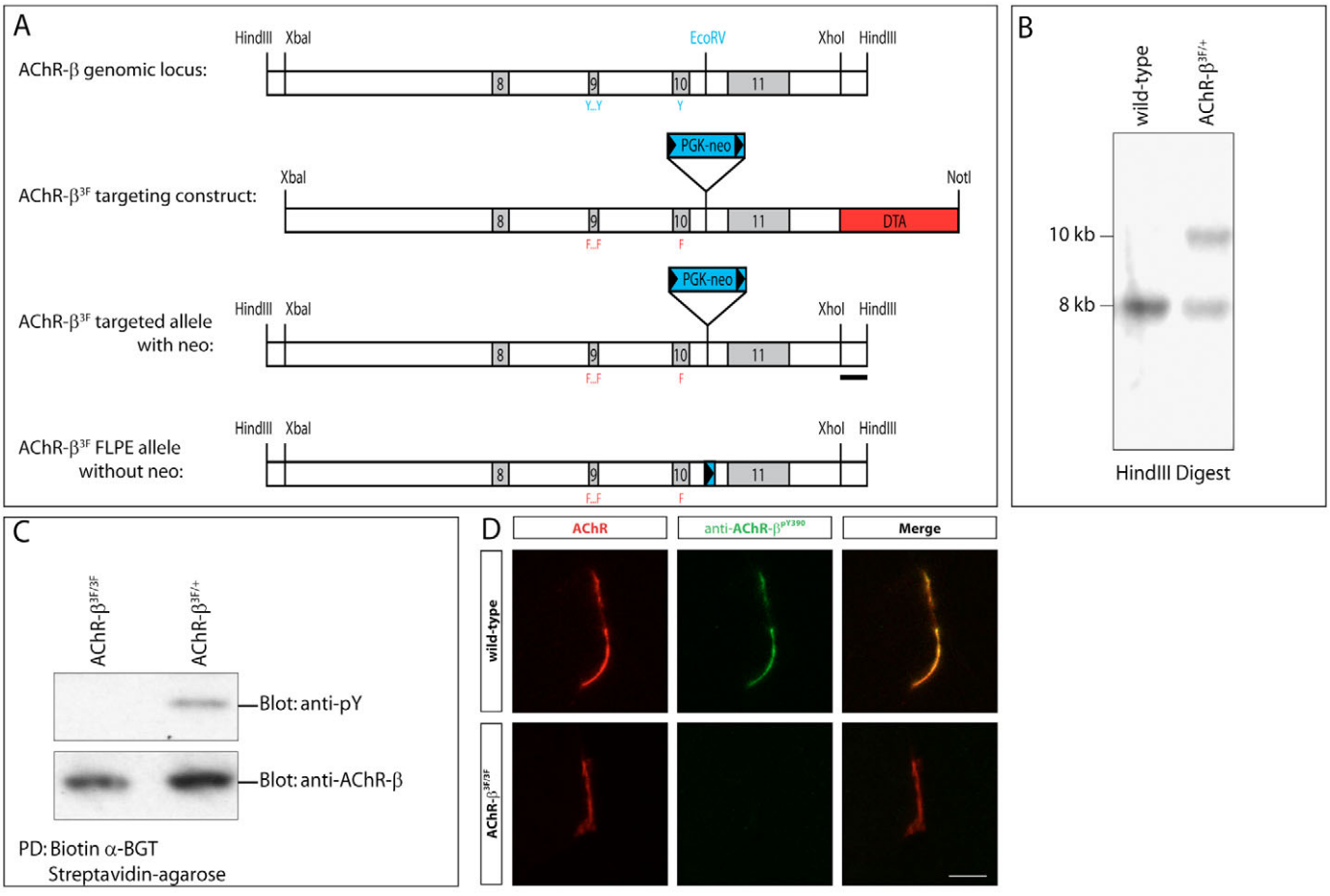

Fig. 1. Generation of mice lacking tyrosine phosphorylation sites in the AChR β-subunit. (**A**) The structures of the AChR β-subunit gene, the targeting construct and the targeted locus. (**B**) Southern blots of genomic DNA, which were digested with *Hin*dIII, were hybridized with a probe (indicated in A) that is 3′ to the targeting construct. The labeled band in the targeted allele is 2 kb larger than in wild-type DNA because of the insertion of the PGK-neo cassette. (**C**) Western blots of AChRs, isolated with biotin-conjugated α-BGT, were probed with antibodies to phosphotyrosine. The AChR β-subunit is tyrosine phosphorylated in wild-type but not in *AChR-β$^{3F/3F}$* mice. (**D**) Sections of skeletal muscle from P30 *AChR-β$^{3F/3F}$* and wild-type mice were stained with Alex Fluor 594-α-BGT and antibodies against a phosphopeptide specific to AChR-β$^{Y390\text{-}P}$. Antibodies to AChR-β$^{Y390\text{-}P}$ label synaptic sites in wild-type but not in *AChR-β$^{3F/3F}$* mice. Scale bar: 10 μm.

Alexa594-α-BGT to label postsynaptic AChRs and antibodies to Neurofilament and Synaptophysin to label presynaptic axons and nerve terminals. Fig. 2 shows that AChRs at synapses in wild-type and *AChR-β$^{3F/3F}$* mice are organized in small ovoid plaques, apposed by nerve terminals, indicating that this simple arrangement of AChRs at developing synapses is not dependent upon tyrosine phosphorylation of the AChR β-subunit (Fig. 2A).

In order to determine whether AChRs are clustered at synapses at their normal number and density, we measured the size of synaptic sites and the density of synaptic AChRs in wild-type and *AChR-β$^{3F/3F}$* mutant mice. We found that synaptic size is reduced by ~30% (100±4.7%, *n*=4 for wild-type; 71.1±4.5%, *n*=6 for *AChR-β$^{3F/3F}$* mice), whereas AChR density is unchanged in *AChR-β$^{3F/3F}$* mice (Fig. 2B). These defects in AChR clustering are not due to a decrease in AChR expression, since the total number of surface AChRs, measured by ^{125}I-α-BGT binding, is comparable in *AChR-β$^{3F/3F}$* and wild-type mice (see Fig. S1D in the supplementary material).

The structure of neuromuscular synapses becomes more complex during postnatal development, as ovoid AChR plaques are transformed into complex, pretzel-like shapes, characteristic of adult

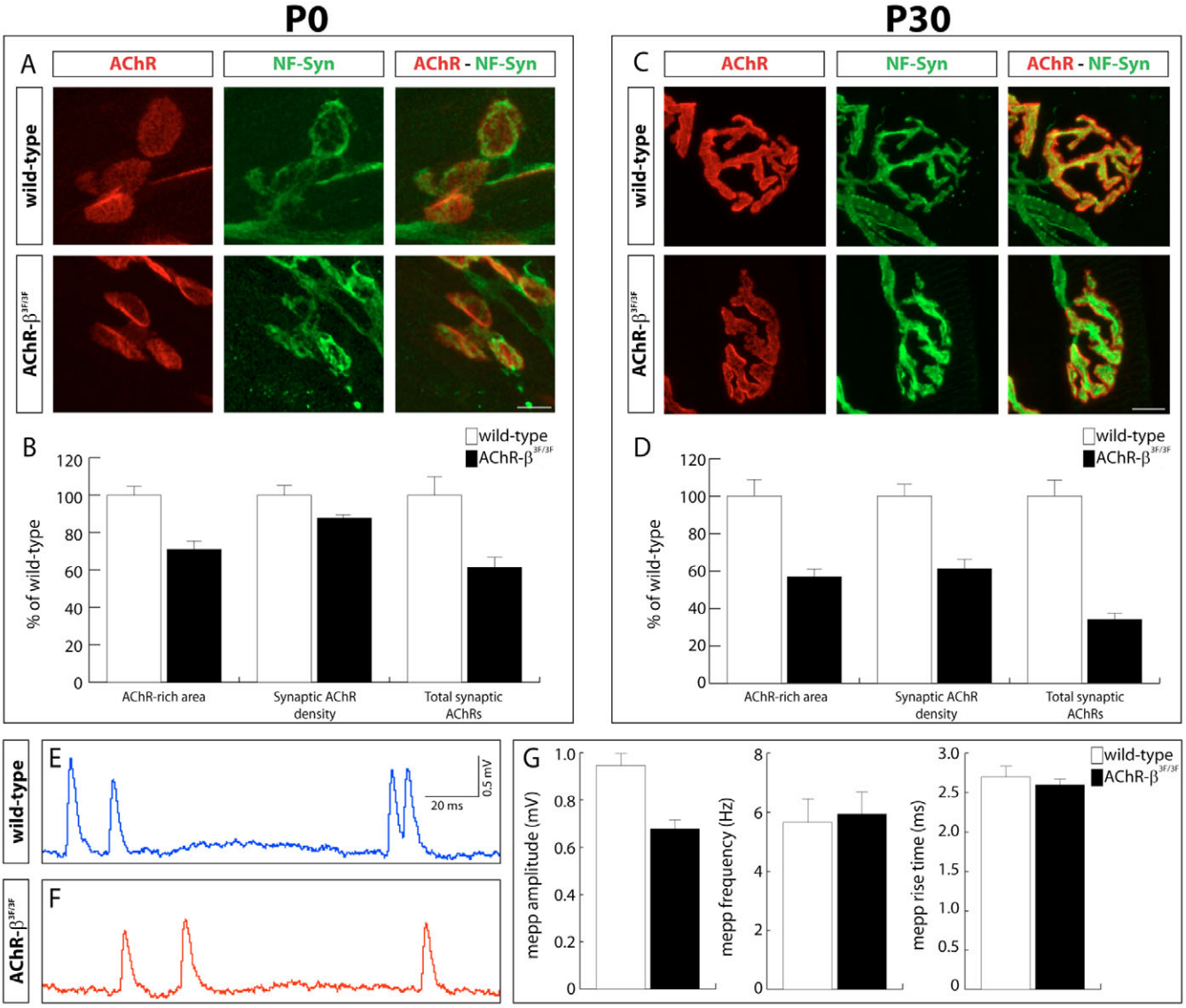

Fig. 2. Synaptic size and AChR density are reduced in *AChR-β$^{3F/3F}$* mice. Whole mounts of diaphragm muscle from P0 (**A**) and P30 (**C**) *AChR-β$^{3F/3F}$* and wild-type mice were stained with Alexa Fluor 594-α-BGT to label AChRs and antibodies to neurofilament and synaptophysin (NF-Syn) to label axons and nerve terminals, respectively. Scale bar: 10 μm. Quantification of AChR area, AChR density and total AChR content at synapses in P0 (**B**) and P30 (**D**) mice. (B) At P0, the synaptic AChR area but not AChR density is reduced in AChR-β$^{3F/3F}$ mice. AChR area: wild type, 100±4.7%, *n*=4; *AChR-β$^{3F/3F}$*, 71.1±4.5%, *n*=6; *P*<0.005; AChR density: wild type, 100±5.2%, *n*=4; *AChR-β$^{3F/3F}$*, 87.8±1.7%, *n*=6; *P*>0.05; total AChR content: wild type, 100±9.9%, *n*=4; *AChR-β$^{3F/3F}$*, 61.4±5.5%, *n*=6; *P*<0.05. (D) At P30, the synaptic AChR area and AChR density are reduced in AChR-β$^{3F/3F}$ mice. AChR area: wild type, 100±8.6%, *n*=3; *AChR-β$^{3F/3F}$*, 56.8±4.1%, *n*=5; *P*<0.05; AChR density: wild type, 100±6.3%, *n*=3; *AChR-β$^{3F/3F}$*, 61.2±5.1%, *n*=5; *P*<0.05; total AChR content: wild type: 100±8.4%, *n*=3; AChR-β$^{3F/3F}$, 34.0±3.3%, *n*=5; *P*<0.05. (**E**,**F**) Miniature end-plate potentials (mepps) were recorded from synapses in diaphragm muscles from P30 *AChR-β$^{3F/3F}$* mice (F) and wild-type (E) littermates. (**G**) The mepp amplitude is significantly reduced in *AChR-β$^{3F/3F}$* mice: wild type, 0.95±0.05 mV, *n*=35; *AChR-β$^{3F/3F}$*, 0.68±0.04 mV, *n*=35; *P*<0.005. The frequency and rise-time of mepps are normal in *AChR-β$^{3F/3F}$* mice. Frequency: wild type, 5.7±0.8 Hz, *n*=35; *AChR-β$^{3F/3F}$*, 6.0±0.7 Hz, *n*=35; *P*>0.05; rise time: wild type, 2.7±0.1 ms, *n*=35; *AChR-β$^{3F/3F}$*, 2.6±0.1 ms, *n*=35; *P*>0.05. All *P* values were calculated using an unpaired *t*-test.

synapses (Sanes and Lichtman, 2001). At P30, synapses in *AChR-β$^{3F/3F}$* mice are ~40% smaller than in wild-type mice (100±8.6%, *n*=3 for wild-type mice; 56.8±4.1%, *n*=5 for *AChR-β$^{3F/3F}$* mice), indicating that the decrease in synaptic size observed at P0 is not caused by a delay in synaptic differentiation (Fig. 2D). In addition, by P30 the density of synaptic AChRs is also reduced by ~40% (100±6.3%, *n*=3 for wild-type mice; 61.2±5.1%, *n*=5 for *AChR-β$^{3F/3F}$* mice), leading to an approximately threefold reduction in the total number of AChRs at each synapse (Fig. 2D).

Since miniature end-plate potential (mepp) size is proportional to the density of synaptic AChRs, we measured the size and frequency of mepps in muscle from wild-type and *AChR-β$^{3F/3F}$* mutant mice in order to obtain a second, independent measure of AChR density. Fig. 2E-G shows that the frequency of mepps is comparable in mutant and control mice, whereas the amplitude of mepps is reduced by ~30% in *AChR-β$^{3F/3F}$* mutant mice (0.95±0.05 mV, *n*=35 synapses from wild-type mice; 0.68±0.04 mV, *n*=35 synapses from *AChR-β$^{3F/3F}$* mice). Thus, these data demonstrate that AChR β-subunit tyrosine phosphorylation is critical to cluster AChRs at their normal number and density at synaptic sites.

Morphological aberrations in *AChR-β$^{3F/3F}$* synapses

Concomitant with the formation of a complex, pretzel-shaped terminal arbor, the postsynaptic membrane becomes invaginated into deep and regularly spaced postjunctional folds (Salpeter, 1987). AChRs are concentrated at the crests and along the upper portions of these postjunctional folds (Fertuck and Salpeter, 1976). When viewed en-face by light microscopy, this arrangement leads to a regular, striped appearance of AChRs at neuromuscular synapses (Anderson and Cohen, 1974). To determine whether AChR β-subunit tyrosine phosphorylation is necessary for this aspect of postsynaptic development, we collected confocal images of synapses, stained with Alexa Fluor 594-α-BGT and compared the organization of AChRs at wild-type and *AChR-β$^{3F/3F}$* mutant synapses in P30 mice (Fig. 3A-H). At synapses in wild-type mice, the synaptic area is organized into well-defined AChR stripes. Moreover, most synaptic branches contain few (two or less) gaps in AChR-rich areas (Fig. 3I,J). In contrast, the synaptic area in *AChR-β$^{3F/3F}$* mice is largely devoid of well-defined AChR stripes, and most terminal branches are interrupted by five or more gaps in AChR staining. These aberrations in synaptic morphology suggest that tyrosine phosphorylation of AChR β-subunit is necessary for the normal development and/or maintenance of neuromuscular cytoarchitecture.

These alterations in AChR organization could be caused by defects in the formation of postjunctional folds. To investigate this possibility we examined the structure of neuromuscular synapses from P30 wild-type and *AChR-β$^{3F/3F}$* mice by electron microscopy. The organization of the neuromuscular junction in *AChR-β$^{3F/3F}$* mice appears largely normal (Fig. 3K-N): first, nerve terminals contain synaptic vesicles, some of which are focused across from the mouths of postjunctional folds; second, the synaptic basal lamina is interposed between presynaptic and postsynaptic membranes; third, postjunctional folds, which are lined by basal lamina, are readily apparent; fourth, the crests and upper portions of the postjunctional folds are often thick and darkly stained, probably because of the dense packing of AChRs (Fertuck and Salpeter, 1976) (Fig. 3M,N). We quantified the number of postjunctional folds in three ways: first, we calculated a fold-density by dividing the number of postjunctional folds, defined by invaginations lined with basal lamina, independent of whether these invaginations had visible mouths that open to the synaptic cleft, by the length of the synaptic cleft; second, we calculated a fold-index by dividing the total length of postjunctional fold membrane, independent of whether these folds had visible mouths that open to the synaptic cleft, by the length of the synaptic cleft; third, we calculated the density of postjunctional folds with openings, or mouths, to the synaptic cleft (Fig. 3O). According to the first and second methods, the number and length of postjunctional folds are normal in *AChR-β$^{3F/3F}$* mutant mice. According to the third method, however, the number of postjunctional folds is reduced by ~40% (0.38±0.02 mouths/μm, *n*=57 for wild-type mice; 0.24±0.01 mouths/μm, *n*=75 for *AChR-β$^{3F/3F}$* mice; Fig. 3O). Thus, in *AChR-β$^{3F/3F}$* mutant mice, postjunctional folds have fewer openings to the synaptic cleft than in wild-type mice, although the entire length of fold membrane appears normal (Fig. 3P,Q).

Localization of proteins to the postsynaptic membrane in *AChR-β$^{3F/3F}$* mice

Agrin stimulates the clustering of multiple synaptic proteins, in addition to AChRs, in cultured myotubes, raising the possibility that the accumulation of these proteins at synapses may depend upon AChR β-subunit tyrosine phosphorylation. We stained frozen sections of muscle from P30 mice with antibodies to adenomatous polyposis coli (APC), rapsyn, MuSK, Abl1, utrophin and dystroglycan and found that each of these proteins is concentrated at synaptic sites in *AChR-β$^{3F/3F}$* mice (Fig. 4). Thus, the accumulation of these postsynaptic proteins at synapses is not dependent upon AChR β-subunit tyrosine phosphorylation.

Attenuation of AChR clustering in *AChR-β$^{3F/3F}$* myotubes

To determine whether tyrosine phosphorylation of the AChR β-subunit has a role in clustering AChRs in response to agrin, we generated muscle cell lines from wild-type and *AChR-β$^{3F/3F}$* mice and examined their response to agrin. We stimulated wild-type and *AChR-β$^{3F/3F}$* myotubes with agrin for 16 hours, labeled AChRs with Alexa Fluor 594-α-BGT, and measured the number and size of AChR clusters (Fig. 5A). The number of spontaneous, agrin-independent AChR clusters is similar in mutant and wild-type myotubes (Fig. 5B). Agrin stimulation induces a ~3.5-fold increase in the number of AChR clusters in wild-type myotubes but smaller, ~1.4-fold increase in the number of AChR clusters in *AChR-β$^{3F/3F}$* myotubes (Fig. 5B). Wild-type and *AChR-β$^{3F/3F}$* myotubes contain large and small AChR clusters, and the number of AChR clusters of all sizes is reduced in *AChR-β$^{3F/3F}$* mutant myotubes (Fig. 5B). These results indicate that tyrosine phosphorylation of the AChR β-subunit is not required to cluster AChRs per se, but is necessary to fully respond to agrin and to maximally cluster AChRs.

Agrin does not stabilize AChRs in *AChR-β$^{3F/3F}$* myotubes

Agrin treatment slows the rate of AChR extraction with non-ionic detergent, suggesting that agrin stimulation leads to a more stable association of AChRs with the cytoskeleton (Wallace, 1992; Borges and Ferns, 2001; Moransard et al., 2003). To determine whether tyrosine phosphorylation of the AChR β-subunit is necessary to stabilize AChRs, we treated wild-type and *AChR-β$^{3F/3F}$* myotubes with agrin for 3 hours, labeled AChRs with ^{125}I-α-BGT for 1 hour in the presence of agrin, extracted labeled AChRs with non-ionic detergent for several minutes and measured the rate of AChR extraction. In wild-type myotubes, agrin stimulation causes a decrease in the rate of AChR extraction (Fig. 5C). By contrast, in

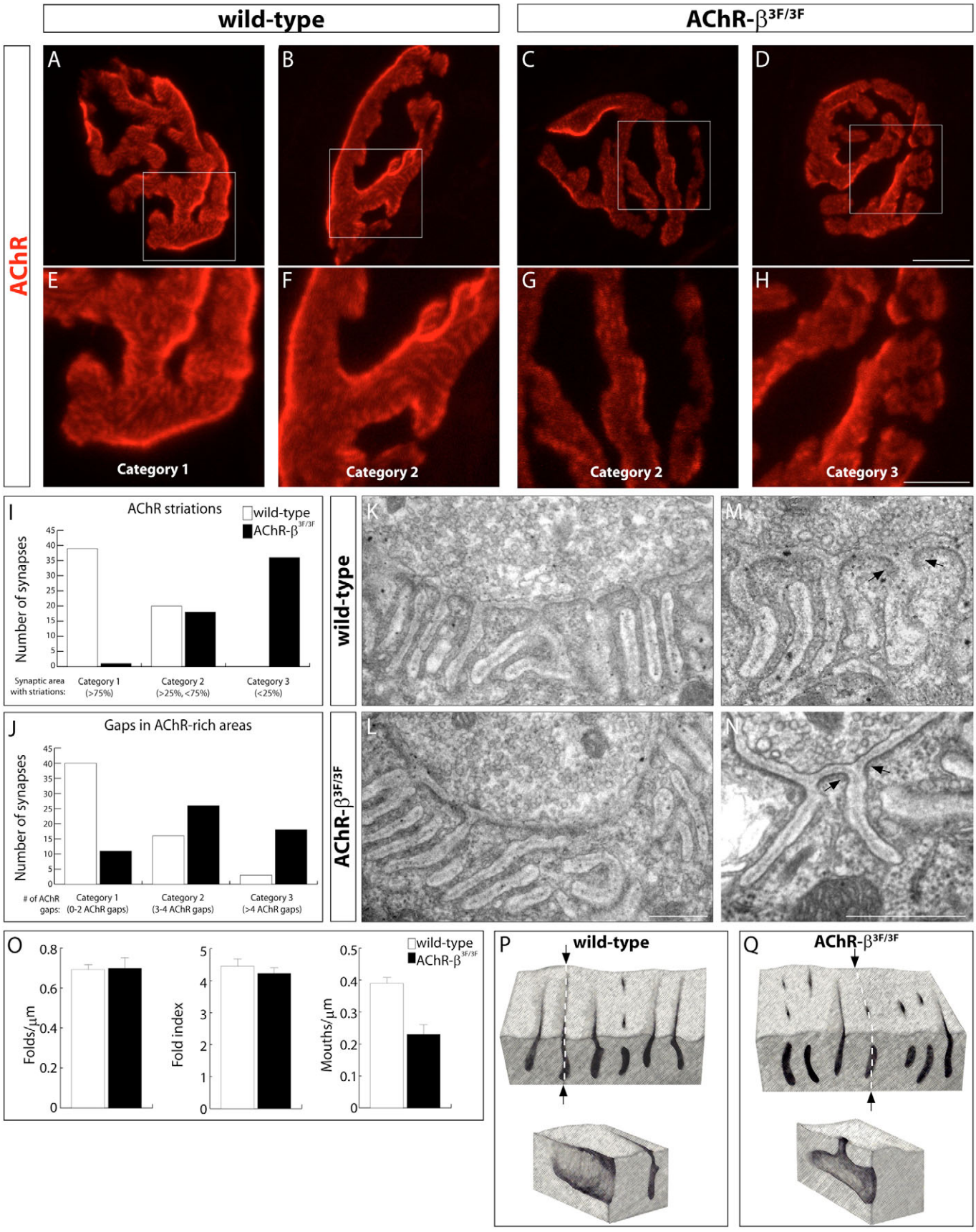

Fig. 3. See next page for legend.

Fig. 3. *AChR-β$^{3F/3F}$* mice fail to form morphologically complex synapses. (**A-H**) Confocal images of synapses, stained with Alexa Fluor 594-α-BGT, in the diaphragm muscle from P30 wild-type and *AChR-β$^{3F/3F}$* mice. E-H are higher magnification images of the boxed regions in A-D. Scale bar: 10 μm for A-D and 5 μm for E-H. (**I**) At category 1 synapses, >75% of the surface area is covered with AChR striations; at category 2 synapses, 25-75% of the surface area is covered with AChR striations; at category 3 synapses, <25% of the surface area is covered with AChR striations. *AChR-β$^{3F/3F}$* mice have fewer category 1 synapses and more category 3 synapses than wild-type mice. Wild type: 39 category 1 synapses, 20 category 2 synapses, 0 category 3 synapses; *AChR-β$^{3F/3F}$*: 1 category 1 synapse, 18 category 2 synapses, 36 category 3 synapses; $P<0.005$, χ^2 test. (**J**) Two or fewer gaps are evident at category 1 synapses; three or four gaps are evident at category 2 synapses; five or more gaps are evident at category 3 synapses. *AChR-β$^{3F/3F}$* mice have fewer category 1 synapses and more category 3 synapses than wild-type mice. Wild type: 40 category 1 synapses, 16 category 2 synapses, 3 category 3 synapses; *AChR-β$^{3F/3F}$*: 11 category 1 synapses, 26 category 2 synapses, 18 category 3 synapses; $P<0.005$, χ^2 test. (**K-N**) Ultrastructural analysis of wild-type and *AChR-β$^{3F/3F}$* mice. (K,L) Presynaptic nerve terminals in wild-type (K) and *AChR-β$^{3F/3F}$* (L) mice are filled with synaptic vesicles and are apposed by postjunctional folds. Scale bar: 500 nm. (M,N) The postsynaptic membrane in wild-type (M) and *AChR-β$^{3F/3F}$* (N) mice is electron dense at the tops of the postjunctional folds (arrows). Scale bar=500 nm. (**O**) The number of total postjunctional folds and the fold index are normal in *AChR-β$^{3F/3F}$* mice, but the number of openings, or mouths, to the synaptic cleft is reduced in *AChR-β$^{3F/3F}$* mice. Number of total postjunctional folds: wild type, 0.69±0.04 folds/μm, $n=57$; *AChR-β$^{3F/3F}$*, 0.70±0.03 folds/μm, $n=75$; $P>0.05$, unpaired *t*-test. The fold index: wild type, 4.5±0.2, $n=57$; *AChR-β$^{3F/3F}$*, 4.2±0.2%, $n=75$; $P>0.05$, unpaired *t*-test. The number of postjunctional fold mouths: wild type, 0.38±0.02 mouths/μm, $n=57$; *AchR-β$^{3F/3F}$*, 0.24±0.01 mouths/μm, $n=75$; $P<0.005$. (**P**,**Q**) A model to illustrate the organization of postjunctional folds in wild-type (P) and *AChR-β$^{3F/3F}$* (Q) mice. In *AChR-β$^{3F/3F}$* mice, the number of postjunctional folds, lined with basal lamina, is normal, but fewer postjunctional folds have mouths that open to the synaptic cleft; as a consequence, the number of AChR striations is reduced in *AChR-β$^{3F/3F}$* mice (E,F versus G,H).

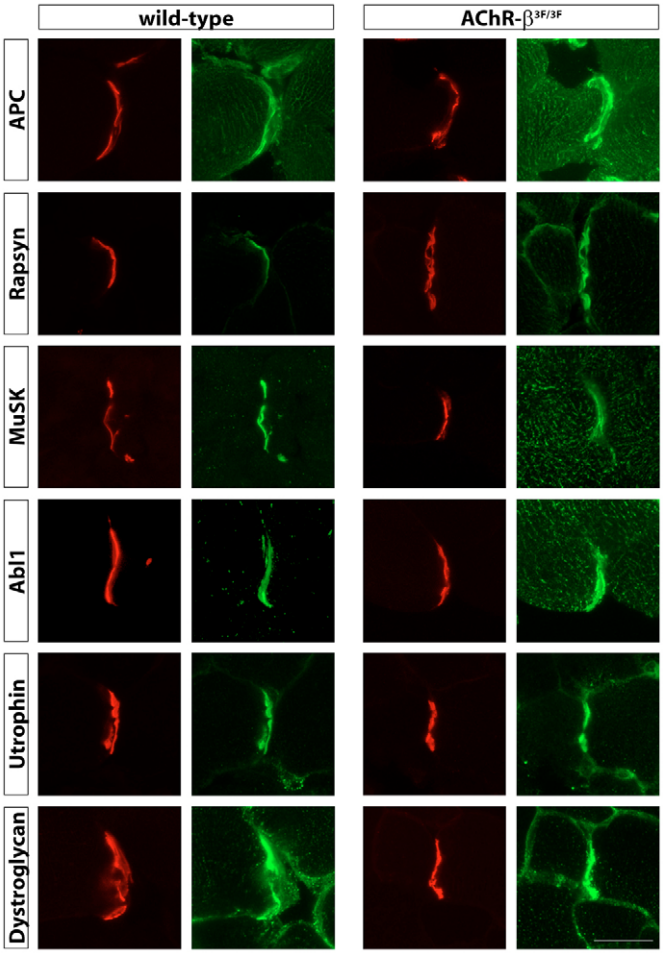

Fig. 4. Postsynaptic proteins are concentrated at synapses in *AChRβ$^{3F/3F}$* mice. Frozen sections of hindlimb muscles from P30 wild-type and *AChRβ$^{3F/3F}$* mice were stained with Alexa Fluor 594-α-BGT to label AChRs (red) and antibodies to APC, rapsyn, MuSK, Abl, utrophin, and dystroglycan (green). Each protein is concentrated at synapses in wild-type and *AChRβ$^{3F/3F}$* mice. The image levels for *AChRβ$^{3F/3F}$* mutant synapses were adjusted so that staining for AChR and other synaptic proteins was clearly visible. Scale bar: 20 μm.

AChR-β$^{3F/3F}$ myotubes, agrin does not alter the rate of AChR extraction (Fig. 5C), indicating that tyrosine phosphorylation of the AChR β-subunit is necessary to stabilize AChRs following agrin stimulation. Moreover, staurosporine treatment destabilizes AChRs in wild-type myotubes but fails to accelerate the rate of AChR extraction from *AChR-β$^{3F/3F}$* myotubes, indicating that staurosporine destabilizes AChRs by inhibiting tyrosine phosphorylation of the AChR β-subunit (Fig. 5C).

DISCUSSION

Agrin stimulation leads sequentially to MuSK tyrosine phosphorylation, AChR tyrosine phosphorylation and AChR clustering. Tyrosine phosphorylation of MuSK and clustering of AChRs are essential for the formation and function of neuromuscular synapses, but the role of AChR tyrosine phosphorylation in synapse formation had not been previously examined. Here, we show that tyrosine phosphorylation of the AChR β-subunit is necessary to form normal neuromuscular synapses. In the absence of AChR β-subunit tyrosine phosphorylation, developing synapses are smaller. Synaptic abnormalities become more profound as synapses mature, since synapses in postnatal mice are not only smaller, but also have a reduced density and an aberrant arrangement of synaptic AChRs and postjunctional folds. Nonetheless, mice lacking AChR β tyrosine phosphorylation move and breathe normally, indicating that tyrosine phosphorylation of the AChR β-subunit is not an essential step in forming or maintaining functional neuromuscular synapses. The absence of behavioral defects in *AChR-β$^{3F/3F}$* mutant mice is probably the result of the large safety factor for synaptic transmission at neuromuscular synapses: although synapses in *AChR-β$^{3F/3F}$* mutant mice contain three-fold fewer AChRs than in wild-type mice, neuromuscular synapses contain four- to five-fold more AChRs than required to sustain synaptic transmission (Wood and Slater, 2001). Below, we discuss the implications of these results: first, the role of AChR β-subunit tyrosine phosphorylation in clustering AChRs at synapses; second, the unexpected finding that synapses are smaller in mice lacking AChR β tyrosine phosphorylation; third, the role of AChR β-subunit tyrosine phosphorylation in linking AChRs to the cytoskeleton and organizing postjunctional folds.

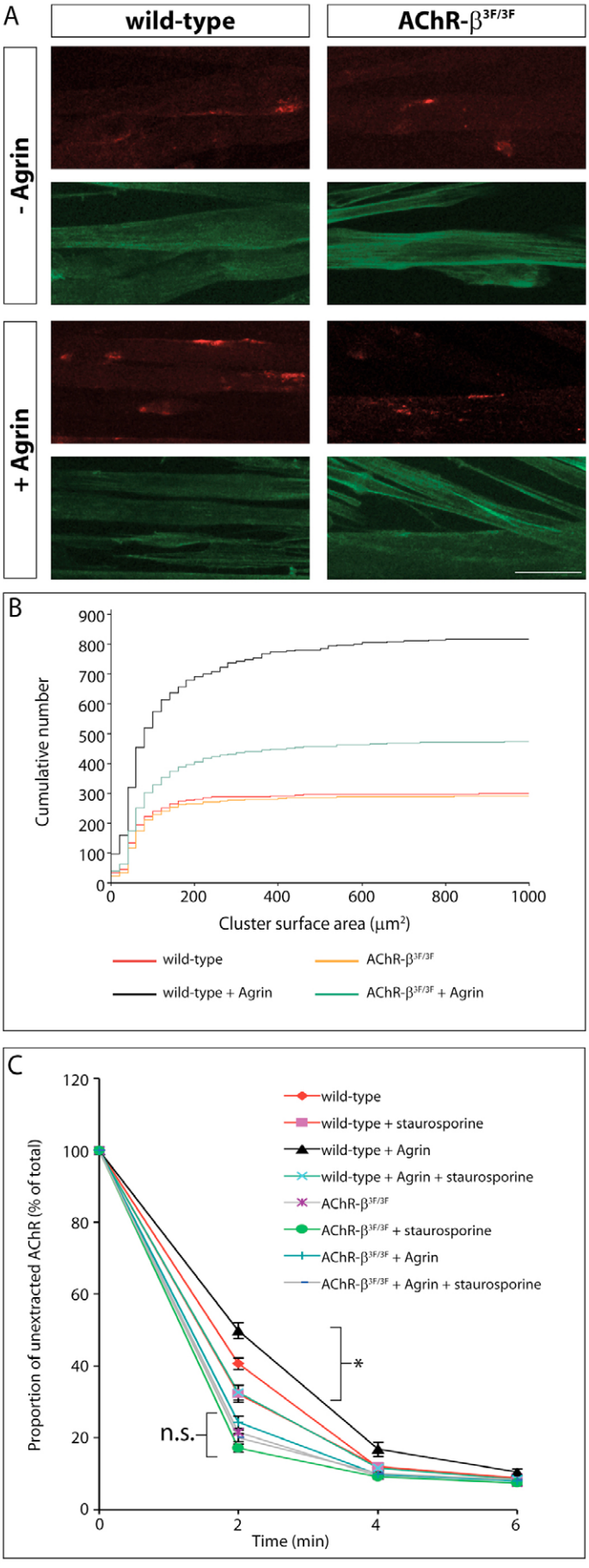

Fig. 5. AChR clustering and stabilization are defective in *AChR-β$^{3F/3F}$* myotubes. (**A**) Agrin-induced AChR clustering is attenuated in *AChR-β$^{3F/3F}$* muscle fibers. Wild-type and *AChR-β$^{3F/3F}$* myotubes were treated with agrin, and AChRs were labeled with Alexa Fluor 594-α-BGT. Scale bar: 50 μm. (**B**) Quantification of AChR cluster size and number in wild-type and *AChR-β$^{3F/3F}$* myotubes. The size and number of AChR clusters that form independent of agrin are similar in wild-type and *AChR-β$^{3F/3F}$* myotubes ($P>0.05$, Mann-Whitney). Agrin induces a 3.5-fold increase in the number of AChR clusters in wild-type myotubes, and a 1.4-fold increase in *AChR-β$^{3F/3F}$* myotubes ($P<0.05$, Mann-Whitney). (**C**) Wild-type and *AChR-β$^{3F/3F}$* myotubes were treated with or without agrin, and AChRs were labeled with ^{125}I-α-BGT. Myotubes were incubated in medium containing 0.05% Triton X-100, which was collected and replaced every 2 minutes for a total of 6 minutes. The amount of ^{125}I-α-BGT extracted at each time point, and the amount remaining bound to the myotubes at the end of the extraction period, was determined. In wild-type myotubes, agrin treatment leads to a significant decrease in the rate of AChR extraction ($P<0.05$, ANOVA), which is abolished when the cells are pretreated with 20 nM staurosporine. Detergent extraction of AChRs from *AChR-β$^{3F/3F}$* muscle fibers is significantly faster than from wild-type fibers (*$P<0.05$) and is not altered by either agrin or staurosporine treatment ($P>0.05$ is considered not significant; n.s.).

AChR β-subunit tyrosine phosphorylation has a role in clustering AChRs at synapses

Previous studies showed that AChR pentamers that contain a mutant β-subunit, which cannot be tyrosine phosphorylated, cluster two-fold less efficiently than wild-type AChRs (Borges and Ferns, 2001). Because the myotubes analyzed in these studies co-expressed wild-type as well as mutant AChR β-subunit, it remained possible that the wild-type AChR pentamers formed a scaffold that facilitated the clustering of mutant AChR pentamers and obscured a more dramatic role of AChR β tyrosine phosphorylation in clustering AChRs. We find that AChR clustering is reduced to a similar extent (2.5-fold reduction) in myotubes that express only mutant AChR pentamers. Thus, AChR β-subunit tyrosine phosphorylation contributes to, but is not essential for, AChR clustering.

We cannot exclude the possibility, however, that tyrosine phosphorylation of the β- and δ-subunits have redundant roles and that tyrosine phosphorylation of the AChR is essential for clustering AChRs. Nonetheless, the tyrosine phosphorylation sites in the β- and δ-subunits are embedded in different sequences, indicating that the phosphorylated subunits are unlikely to recruit the same adaptor protein (Colledge and Froehner, 1997). Notably, the tyrosine phosphorylation site in the δ-subunit conforms to a binding site for SH2 domains, whereas the tyrosine phosphorylation site in the β-subunit is not predicted to bind SH2 or PTB domains. For this reason, phosphorylation of the different subunits is unlikely to have a redundant role.

In wild-type myotubes, agrin induces the formation of AChR micro-clusters, in a Rac-dependent manner, and AChR macro-clusters, in a Rho-dependent manner (Weston et al., 2000; Weston et al., 2003). We find that the number of micro- and macro-clusters are reduced to the same extent in *AChR-β$^{3F/3F}$* mutant myotubes. Our findings are consistent with two possibilities: (1) Rac- and Rho-dependent pathways each

depend upon *AChR-β$^{3F/3F}$* tyrosine phosphorylation or (2) micro- and macro-clusters are similarly unstable in the absence of *AChR-β$^{3F/3F}$* tyrosine phosphorylation.

Synapses are smaller in mice lacking AChR β tyrosine phosphorylation

Because AChRs containing a mutant AChR β-subunit cluster less efficiently in cultured myotubes (Borges and Ferns, 2001) (Fig. 5A,B), we were not surprised to find that the density of AChRs is reduced at synapses in *AChR-β$^{3F/3F}$* mutant mice. We did not anticipate, however, that synaptic size would be reduced in *AChR-β$^{3F/3F}$* mutant mice. Notably, the density of synaptic AChRs is reduced in utrophin mutant mice, yet the size of utrophin-deficient neuromuscular synapses is normal (Deconinck et al., 1997; Grady et al., 1997). Thus, a reduction in the density, or packing of synaptic AChRs, does not necessarily lead to a reduction in synaptic size. Neuromuscular synapses are smaller but contain a normal density of synaptic AChRs in humans carrying mutations in *DOK7* (Beeson et al., 2006; Slater et al., 2006). DOK7 is an adaptor protein that is recruited to tyrosine phosphorylated MuSK and necessary for signaling downstream from MuSK, including AChR tyrosine phosphorylation (Okada et al., 2006). Thus, it is possible that a failure to phosphorylate AChRs in patients harboring *DOK7* mutations is responsible for the decrease in synaptic size.

The role of AChR β-subunit tyrosine phosphorylation in linking AChRs to the cytoskeleton and organizing postjunctional folds

Our studies in *AChR-β$^{3F/3F}$* muscle cell lines suggest that the defects in AChR clustering at synapses may be caused, at least in part, by a failure to link mutant AChRs to an underlying cytoskeleton. Rapsyn, which is essential for clustering AChRs, binds the AChR β-subunit and associates more efficiently with AChRs following agrin stimulation (Burden et al., 1983; Gautam et al., 1995; Moransard et al., 2003). APC is also reported to bind the AChR β-subunit, to associate more efficiently with AChRs following agrin stimulation, and to be required for clustering AChRs in cultured muscle cells (Wang et al., 2003). Although these data raise the possibility that alterations in the binding of rapsyn and/or APC to AChRs might underlie the synaptic defects observed in *AChR-β$^{3F/3F}$* mice, we find that APC and rapsyn are concentrated at synaptic sites in the absence of AChR β-subunit tyrosine phosphorylation. Although we cannot exclude the possibility that reduced amounts of rapsyn and/or APC are present at synapses in *AChR-β$^{3F/3F}$* mutant mice, these data demonstrate that the accumulation of rapsyn and APC at synapses does not depend upon AChR β-subunit tyrosine phosphorylation.

The reductions in AChR density and postjunctional fold formation in *AChR-β$^{3F/3F}$* mice are strikingly similar to the synaptic defects observed in utrophin mutant mice (Deconinck et al., 1997; Grady et al., 1997). Utrophin and AChRs colocalize at the tops of postjunctional folds and form a complex in cultured muscle fibers (Bewick et al., 1992; Fuhrer et al., 1999). These data suggest that tyrosine phosphorylation of the AChR β-subunit and utrophin might function in the same pathway. Utrophin, however, remains concentrated at synapses in *AChR-β$^{3F/3F}$* mice, and the AChR β-subunit is tyrosine phosphorylated in utrophin mutant mice (data not shown). Thus, these data do not support the idea that the defects in *AChR-β$^{3F/3F}$* mice are due to a failure to recruit utrophin or that the synaptic defects in utrophin mutant mice are due to a lack of AChR β-subunit tyrosine phosphorylation.

How might tyrosine phosphorylation of the AChR β-subunit regulate the formation of postjunctional folds? Our data are consistent with the possibility that tyrosine phosphorylation of the AChR β-subunit provides a docking site for a protein(s) that is involved in forming and/or stabilizing postjunctional folds. Alternatively, others have suggested that the dense packing of conically shaped AChRs may be sufficient to induce folding of the postsynaptic membrane (Unwin, 2005) raising the possibility that the reduced density of synaptic AChRs in *AChR-β$^{3F/3F}$* mice might lead to a reduction in the number of postjunctional folds (Slater et al., 1997).

Interestingly, synapses in patients carrying mutations in *DOK7* have fewer postjunctional folds (Beeson et al., 2006; Slater et al., 2006). Since tyrosine phosphorylation of the AChR β-subunit depends upon DOK7, these findings raise the possibility that the reduced number of postjunctional folds in patients harboring mutations in *DOK7* may be due, at least in part, to a failure to fully tyrosine phosphorylate the AChR β-subunit (Okada et al., 2006).

We are grateful to Jon Lindstrom for providing a monoclonal antibody (mAb124) to the AChR β-subunit, to Doju Yoshikami for helpful advice and to Kevin Campbell for kindly providing utrophin$^{-/-}$ tissue and antibodies to dystroglycan. We thank Jihua Fan for excellent technical assistance, Peter Hallock for comments on the manuscript, and Anya Temple for the drawings of postjunctional folds. This work was supported by funds from the NIH (NS 36193) to S.J.B. and a NRSA predoctoral fellowship to M.B.F.

Supplementary material

Supplementary material for this article is available at http://dev.biologists.org/cgi/content/full/134/23/4167/DC1

References

Anderson, M. J. and Cohen, M. W. (1974). Fluorescent staining of acetylcholine receptors in vertebrate skeletal muscle. *J. Physiol.* **237**, 385-400.

Beeson, D., Higuchi, O., Palace, J., Cossins, J., Spearman, H., Maxwell, S., Newsom-Davis, J., Burke, G., Fawcett, P., Motomura, M. et al. (2006). Dok-7 mutations underlie a neuromuscular junction synaptopathy. *Science* **313**, 1975-1978.

Bewick, G. S., Nicholson, L. V., Young, C., O'Donnell, E. and Slater, C. R. (1992). Different distributions of dystrophin and related proteins at nerve-muscle junctions. *NeuroReport* **3**, 857-860.

Borges, L. S. and Ferns, M. (2001). Agrin-induced phosphorylation of the acetylcholine receptor regulates cytoskeletal anchoring and clustering. *J. Cell Biol.* **153**, 1-12.

Burden, S. J., DePalma, R. L. and Gottesman, G. S. (1983). Crosslinking of proteins in acetylcholine receptor-rich membranes: association between the beta-subunit and the 43 kd subsynaptic protein. *Cell* **35**, 687-692.

Colledge, M. and Froehner, S. C. (1997). Tyrosine phosphorylation of nicotinic acetylcholine receptor mediates Grb2 binding. *J. Neurosci.* **17**, 5038-5045.

DeChiara, T. M., Bowen, D. C., Valenzuela, D. M., Simmons, M. V., Poueymirou, W. T., Thomas, S., Kinetz, E., Compton, D. L., Rojas, E., Park, J. S. et al. (1996). The receptor tyrosine kinase MuSK is required for neuromuscular junction formation in vivo. *Cell* **85**, 501-512.

Deconinck, A. E., Potter, A. C., Tinsley, J. M., Wood, S. J., Vater, R., Young, C., Metzinger, L., Vincent, A., Slater, C. R. and Davies, K. E. (1997). Postsynaptic abnormalities at the neuromuscular junctions of utrophin-deficient mice. *J. Cell Biol.* **136**, 883-894.

Fertuck, H. C. and Salpeter, M. M. (1976). Quantitation of junctional and extrajunctional acetylcholine receptors by electron microscope autoradiography after 125I-alpha-bungarotoxin binding at mouse neuromuscular junctions. *J. Cell Biol.* **69**, 144-158.

Fuhrer, C., Gautam, M., Sugiyama, J. E. and Hall, Z. W. (1999). Roles of rapsyn and agrin in interaction of postsynaptic proteins with acetylcholine receptors. *J. Neurosci.* **19**, 6405-6416.

Gautam, M., Noakes, P. G., Mudd, J., Nichol, M., Chu, G. C., Sanes, J. R. and Merlie, J. P. (1995). Failure of postsynaptic specialization to develop at neuromuscular junctions of rapsyn-deficient mice. *Nature* **377**, 232-236.

Glass, D. J., Bowen, D. C., Stitt, T. N., Radziejewski, C., Bruno, J., Ryan, T. E., Gies, D. R., Shah, S., Mattsson, K., Burden, S. J. et al. (1996). Agrin acts via a MuSK receptor complex. *Cell* **85**, 513-523.

Grady, R. M., Merlie, J. P. and Sanes, J. R. (1997). Subtle neuromuscular defects in utrophin-deficient mice. *J. Cell Biol.* **136**, 871-882.

Huganir, R. L., Miles, K. and Greengard, P. (1984). Phosphorylation of the nicotinic acetylcholine receptor by an endogenous tyrosine-specific protein kinase. *Proc. Natl. Acad. Sci. USA* **81**, 6968-6972.

Jat, P. S., Noble, M. D., Ataliotis, P., Tanaka, Y., Yannoutsos, N., Larsen, L. and Kioussis, D. (1991). Direct derivation of conditionally immortal cell lines from an H-2Kb-tsA58 transgenic mouse. *Proc. Natl. Acad. Sci. USA* **88**, 5096-5100.
Jaworski, A. and Burden, S. J. (2006). Neuromuscular synapse formation in mice lacking motor neuron- and skeletal muscle-derived Neuregulin-1. *J. Neurosci.* **26**, 655-661.
Karnovsky, M. J. and Roots, L. (1964). A 'direct-coloring' thiocholine method for cholinesterases. *J. Histochem. Cytochem.* **12**, 219-221.
Meyer, G. and Wallace, B. G. (1998). Recruitment of a nicotinic acetylcholine receptor mutant lacking cytoplasmic tyrosine residues in its beta subunit into agrin-induced aggregates. *Mol. Cell. Neurosci.* **11**, 324-333.
Mittaud, P., Marangi, P. A., Erb-Vogtli, S. and Fuhrer, C. (2001). Agrin-induced activation of acetylcholine receptor-bound Src family kinases requires Rapsyn and correlates with acetylcholine receptor clustering. *J. Biol. Chem.* **276**, 14505-14513.
Moon, I. S., Apperson, M. L. and Kennedy, M. B. (1994). The major tyrosine-phosphorylated protein in the postsynaptic density fraction is N-methyl-D-aspartate receptor subunit 2B. *Proc. Natl. Acad. Sci. USA* **91**, 3954-3958.
Moransard, M., Borges, L. S., Willmann, R., Marangi, P. A., Brenner, H. R., Ferns, M. J. and Fuhrer, C. (2003). Agrin regulates rapsyn interaction with surface acetylcholine receptors, and this underlies cytoskeletal anchoring and clustering. *J. Biol. Chem.* **278**, 7350-7359.
Okada, K., Inoue, A., Okada, M., Murata, Y., Kakuta, S., Jigami, T., Kubo, S., Shiraishi, H., Eguchi, K., Motomura, M. et al. (2006). The muscle protein Dok-7 is essential for neuromuscular synaptogenesis. *Science* **312**, 1802-1805.
Qu, Z. C., Moritz, E. and Huganir, R. L. (1990). Regulation of tyrosine phosphorylation of the nicotinic acetylcholine receptor at the rat neuromuscular junction. *Neuron* **4**, 367-378.
Salpeter, M. M. (1987). *The Vertebrate Neuromuscular Junction*. New York: Liss.
Sanes, J. R. and Lichtman, J. W. (2001). Induction, assembly, maturation and maintenance of a postsynaptic apparatus. *Nat. Rev.* **2**, 791-805.
Slater, C. R., Young, C., Wood, S. J., Bewick, G. S., Anderson, L. V., Baxter, P., Fawcett, P. R., Roberts, M., Jacobson, L., Kuks, J. et al. (1997). Utrophin abundance is reduced at neuromuscular junctions of patients with both inherited and acquired acetylcholine receptor deficiencies. *Brain* **120**, 1513-1531.
Slater, C. R., Fawcett, P. R., Walls, T. J., Lyons, P. R., Bailey, S. J., Beeson, D., Young, C. and Gardner-Medwin, D. (2006). Pre- and post-synaptic abnormalities associated with impaired neuromuscular transmission in a group of patients with 'limb-girdle myasthenia'. *Brain* **129**, 2061-2076.
Smith, C. L., Mittaud, P., Prescott, E. D., Fuhrer, C. and Burden, S. J. (2001). Src, Fyn, and Yes are not required for neuromuscular synapse formation but are necessary for stabilization of agrin-induced clusters of acetylcholine receptors. *J. Neurosci.* **21**, 3151-3160.
Swope, S. L., Moss, S. J., Raymond, L. A. and Huganir, R. L. (1999). Regulation of ligand-gated ion channels by protein phosphorylation. *Adv. Second Messenger Phosphoprotein Res.* **33**, 49-78.
Unwin, N. (2005). Refined structure of the nicotinic acetylcholine receptor at 4A resolution. *J. Mol. Biol.* **346**, 967-989.
Wallace, B. G. (1992). Mechanism of agrin-induced acetylcholine receptor aggregation. *J. Neurobiol.* **23**, 592-604.
Wallace, B. G., Qu, Z. and Huganir, R. L. (1991). Agrin induces phosphorylation of the nicotinic acetylcholine receptor. *Neuron* **6**, 869-878.
Wan, Q., Man, H. Y., Braunton, J., Wang, W., Salter, M. W., Becker, L. and Wang, Y. T. (1997). Modulation of GABAA receptor function by tyrosine phosphorylation of beta subunits. *J. Neurosci.* **17**, 5062-5069.
Wang, J., Jing, Z., Zhang, L., Zhou, G., Braun, J., Yao, Y. and Wang, Z. Z. (2003). Regulation of acetylcholine receptor clustering by the tumor suppressor APC. *Nat. Neurosci.* **6**, 1017-1018.
Weston, C., Yee, B., Hod, E. and Prives, J. (2000). Agrin-induced acetylcholine receptor clustering is mediated by the small guanosine triphosphatases Rac and Cdc42. *J. Cell Biol.* **150**, 205-212.
Weston, C., Gordon, C., Teressa, G., Hod, E., Ren, X. D. and Prives, J. (2003). Cooperative regulation by Rac and Rho of Agrin-induced acetylcholine receptor clustering in muscle cells. *J. Biol. Chem.* **278**, 6450-6455.
Wood, S. J. and Slater, C. R. (2001). Safety factor at the neuromuscular junction. *Prog. Neurobiol.* **64**, 393-429.